THERMAL MODELLING OF FRICTION STIR PROCESS (FSP) AND IDENTIFICATION PARAMETERS

N. Lebaal[1*], D. Chamoret[1], D. Schlegel[1], M. Folea[2]

[1] ICB UMR 6303, CNRS, Univ. Bourgogne Franche-Comté, UTBM, F-90010 Belfort, France

[2] Universitatea Transilvania Brasov, Braşov, Romania

*e-mail: nadhir.lebaal@utbm.fr

Abstract. The Friction Stir Processing (FSP) is an innovative surface engineering method, considered as a green processing technique. A good physical understanding of the process can be reached by the combined efforts of experimental examination and numerical modelling. In this paper, a three-dimensional heat transfer model for FSP is presented. Then, a numerical inverse method that allows to estimate the Coulomb friction coefficient μ combining experimental test, finite element simulations and optimization is developed.

1. Introduction

Friction Stir Processing (FSP) is an innovative surface engineering method which produces a fine recrystallized layer by thermo-mechanical mixing of the surface and subsurface [1]. It is expected to find applications in a variety of automotive and other industrial applications and can be considered as a green processing technique [2]. For instance, in the energy field, it can be used to process or join vanadium alloys and nanoparticle reinforced copper composite materials for fusion reactor applications [3]. What is attractive about FSP is that it can be incorporated in the overall manufacturing cycle as a post-processing step during the machining operation.

FSP is developed based on the principle of friction stir welding (FSW), which is a thermo-mechanical process based on a very simple basic principle: a rotating tool is moved along a workpiece surface while applying an axial load to increase generated heat. The schematic illustration of FSP is shown in Fig.1. The tool serves two primary functions: heating and deformation of workpiece material. The motion of the tool causes severe plastic deformation to achieve microstructure modification by homogenization and refinement [4,5].
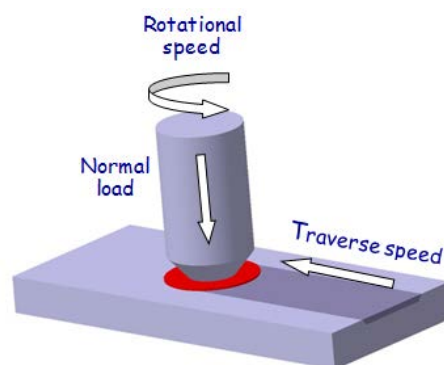

Fig. 1. Friction stir process.

Heat generation and distribution during the process are critical issues, because they can induce microstructural changes.

In this paper, a three-dimensional heat transfer model for friction stir process [6,7] and its finite element solution are presented. The effects of the operating conditions (i.e. translation speed, rotational speed and normal force of the tool) on the temperature distribution are studied.

In particular it will be described a numerical inverse method that allows to estimate the Coulomb friction coefficient by combining experimental test and FE simulation results.

2. Numerical Model

During the Friction Stir Process, the tool moves along the affected zone. This movement would require a fairly complex model if we would like to model the tool as a moving heat source [8], or if we would like to predict the stress field [9]. In this paper a different approach is used: a moving coordinate system is fixed at the tool axis as in reference [10]. After making the coordinate transformation, the heat transfer problem becomes a stationary convection-conduction problem that is straightforward to model. The heat input from the tool is simplified as a moving heat source however, this assumption is not helpful in modeling the coupled heat transfer for both the tool and the workpiece.

Hypothesis. The following main assumptions are made in the presented model:
- The heat generated at the tool shoulder/workpiece interface is frictional heat.
- No heat flows into the workpiece if the local temperature reaches the material melting temperature.
- The model geometry is symmetric around the shoulder. It is therefore sufficient to model only one plate. The plate dimensions are 160 mm-by-60 mm-by-10 mm, surrounded by two infinite domains in the x direction. Fig.2. shows the resulting model geometry.

Heat Transfer during Friction Stir Process. During the main friction stir process, the tool is moving at a constant speed along the joint line. For such a situation, it is well adapted to use a moving coordinate system that moves with the tool, instead of using a stationary system. By applying a moving coordinate, it is not necessary to model the complicated stir process near the shoulder, thus it makes the model easier.
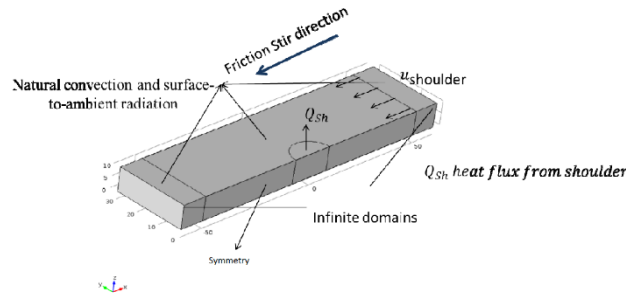

Fig. 2. Hypothesis and numerical model.

The strong form of the balance of energy equation can be written in many different ways, such as:

$$\rho\, C_p\, \frac{d\,T}{dt} = -\overrightarrow{\nabla}.\vec{q} + \dot{\omega} \tag{1}$$

In the above equation:
ρ is the density.
C_p is the specific heat.
T is the temperature.
$\vec{q} = -k\,\nabla T$ is the heat flux.

$\dot{\omega} = [\tau] : [\dot{\varepsilon}]$ is the shear dissipation.

Using the material derivative notion, for constant C_p and k and when $\dot{\omega}$ is neglected, this conservation of energy equation is:

$$\rho \, C_p \, \frac{\partial T}{\partial t} = k \, \Delta T - \rho \, C_p \, \overrightarrow{u} \cdot \overrightarrow{\nabla T} + Q_{sh}, \tag{2}$$

where
k is the thermal conductivity.
$\overrightarrow{u}$ is s the tool moving speed.
Q_{sh} is the heat generated by friction at the tool/workpiece contact surface.

Heat Generation. The main heat source in FSP is generally considered to be the friction between the rotating tool and the workpiece. In this model, the local heat flux generation (caused by the friction) per unit area (W/m2) at the distance R from the center axis of the tool can be calculated by the following expression [7]:

$$Q_{sh}(x, y, T) = \begin{cases} \mu \, F_n \, R(x,y) \, \omega & if \ T < T_{melt} \\ 0 & if \ T > T_{melt} \end{cases}, \tag{3}$$

where R is the distance from the calculated point to the axis of the rotating tool, $\omega = 2\pi r$ is the angular velocity of the tool (rad/s), r is the rotational speed [t/s], F_n is the normal load and μ is the friction coefficient (supposed constant in this model).

Boundary conditions and initial condition.

• Tool shoulder/workpiece interface

The heat flux boundary condition for the workpiece at the tool shoulder/workpiece interface is:

$$k \, \frac{\partial T}{\partial n}\Big|_{\Gamma} = q_{sh} \tag{4}$$

• The convection boundary conditions

The convection boundary condition for all the workpiece surfaces exposed to the air can be expressed as:

$$k \, \frac{\partial T}{\partial n}\Big|_{\Gamma} = h(T - T_0), \tag{5}$$

where n is the normal direction vector of boundary, and h is the convection coefficient. The surface of the workpiece in contact with the backup plate is simplified to the convection condition with an effective convection.

3. Experimental Data

Experimental tests were carried out on samples of a commercial AISI 1045 steel of the following composition (wt.%): 0.45 C, 0.75 Mn, 0.04 P, 0.05 S and Fe bal [11]. Workpiece samples were plates of 160 x 60 x 10 mm. The pinless FSP tool had a cylindrical shape with an 8mm diameter (Figure 3).

Fig. 3. Machine set-up.

A constant rotational speed of 2000 rpm and three different traverse speeds (30, 50, 70 mm/min) and normal loads (900, 1200, 1500 N) were used as processing parameters. The

temperature fields during the process were measured using infrared camera behind the tool. All the processing data and experimental results can be seen in table 1.

Table 1. Experimental results.

Case	Normal Load (N)	Transverse Speed (mm/min)	Friction Time (s)	Measured Temperature (°C)
1		30	160 s	388
2	900	50	96 s	372
3		70	68,6	350
4		30	160 s	458
5	1200	50	96 s	450
6		70	68,6	411
7		30	160 s	489
8	1500	50	96 s	481
9		70	68,6	465

4. Numerical simulation and identification of friction coefficient

Identification parameter. The use of simulation coupled with optimization is a powerful numerical tool to support design in industry and research. This parts deals with the identification of parameters for constitutive models by inverse modeling. The principle of the inverse analysis is as follow: different experimental curves being available from forming experiments, the optimization module is used to run several Finite Element Simulations using various parameter values suggested by the optimization engine. The inverse analysis objective function is simply the least-square error between an experimental and a model data-set.

In this paper, a numerical inverse method [12] that allows to estimate the Coulomb friction coefficient μ combining experimental test and FE simulation results is used. Indeed, heat generation during FSP is mainly due to the friction between tool and workpiece, so a good knowledge of this friction coefficient is a crucial point. To this end, we define the following minimization problem:

$$min\, f(\mu) = \sum_{i=1}^{9} \frac{(\bar{T} - T_{mes})^2}{T_{mes}} \tag{6}$$

$\bar{T}$ is the mean temperature behind the tool calculated on 1 mm. It is evaluated by the Finite Element Method using the thermal model presented in section 2. Simulation parameters are presented in Table 2. T_{mes} is the temperature measured and presented in table 1.

For model parameters identification, many optimization algorithms and tools can be used [13,14]. In this paper, the Pattern Search algorithm is used [15]. This approach is of a great interest because it is robust and can deal successfully with a wide range of problem areas. Moreover, it does not require gradient information, only objective function evaluations. This point is very suitable for problems for which it is impossible to evaluate the derivatives as it is the case here.

Table 2. Simulation parameters (AISI 1045).

k	Thermal conductivity	W/m°C	47,7
ρ	Density	g/cm^3	7,8
C_p	Specific heat	J/Kg/ m°C	432,6
μ	Coefficient of friction		0,1-0.45

5. Results and discussion

Figure 4 shows the calculated temperature field for a constant axial force of 1500N and a low tool speed u=30 mm/min (feed rates). The temperature is highest in the contact zone between

the rotating tool and the workpiece. Behind the tool, the process transports hot material away, while in front of the tool, new cold material enters.
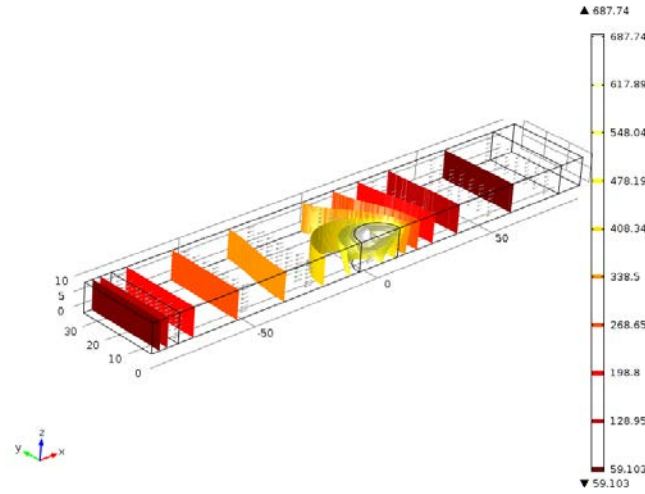

Fig. 4. Temperature field for u=30 mm/min and F=1500 N.

Figure 5 illustrates the temperature history with u=30 mm/min and F=1500 N in two different cases: stationary study and transient study. Concerning the stationary case, it can be noticed that this low tool speed generates high temperature (Black dashed line). However, in the transient case, the temperature field depends on the time. This time is linked to the tool speed (Table 1). To reach this high field temperature (corresponding to stationary study), the friction time needs to be increased.

In Figure 6 (u=70 mm/min and F=1500 N), for the stationary case, it can be noticed that the high tool speed generates low temperatures (Black dashed line), compared to the stationary study case of low tool speed (u=30 mm/min). Nevertheless, this temperature field is higher than the transient case. In the transient case, for the last friction time, the temperature field is not different closely behind the tool, compared to the stationary study. When the distance behind the rotating tool increases, the process transports hot material away and the temperature field decreases. To reach this highest temperature field (corresponding to stationary study), the required friction time must be increased. Because the mean temperature is obtained closely behind the tool the experimental friction time, gives the same results as the stationary results.
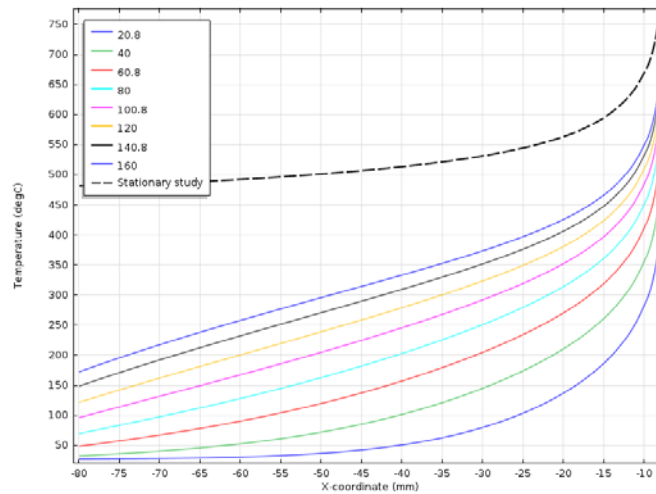

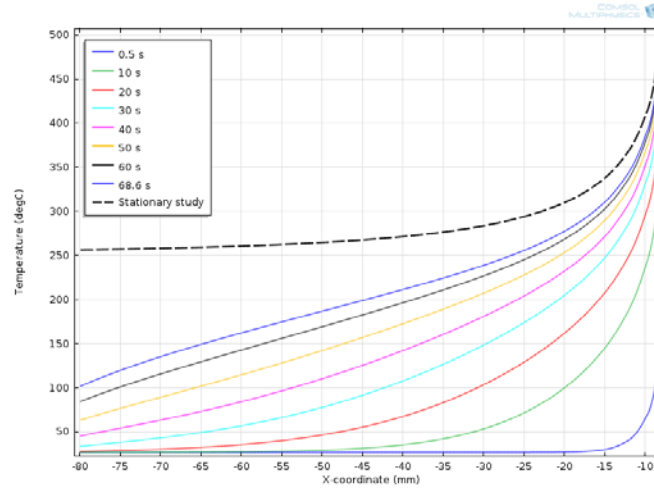**Fig. 5.** Temperature History along the processing line for u=30 mm/min and F=1500 N.

Fig. 6. Temperature History along the processing line for u=70 mm/min and F=1500 N.

To process the inverse analysis, the temperature field of the transient study at last time (table 1) has been considered. The initial value of the friction coefficient is 0.1. For this coefficient, it can be noticed an important gap between measured data and numerical results (Figure 7). The optimized value obtained by the inverse analysis is 0.346. Figure 7 shows the comparison between the numerical temperatures before (blue) and after optimization (purple) and, the experimental results. It can be observed that when the axial force increases and the tool speed is low, the calculated temperatures are higher than the experimental ones. However, for the other data, comparison between the optimized temperatures and measured temperatures are very similar. We can conclude that the optimized numerical results are good results. This method can then allow us to predict other properties of the material, such as grain refinement and microhardness, via numerical methods [16].
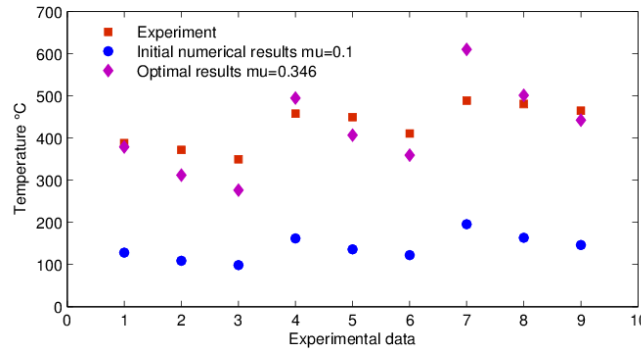

Fig. 7. Comparison between Optimal Temperatures and Experimental temperatures.

6. Conclusion

Friction stir processing of commercially available AISI 1045 steel was studied by investigation through three-dimensional transient heat-transfer model in a moving coordinate and comparison with experimental data.

From an experimental point of view, it was very difficult to obtain the temperature distribution near the moving tool. In order to evaluate the better experimental temperature as possible, the temperature fields during the process were measured using infrared camera behind the tool.

From a numerical point of view, two studies were investigated: stationary and transient heat-transfer study.

We have noticed the stationary state is reached very quickly. This point can be interesting in an optimization context to reduce the simulation time.

The calculated results successfully demonstrated the heat transfer process of the workpiece in friction stir process. The main objective of our work was to well understand the process and to have an idea of the influence and the links between the different process parameters.

The friction coefficient is identified using an optimization algorithm coupled with the simulation software COMSOL multi-physics. The comparison between optimal calculated results and experimental one, gives a good agreement. This model can accurately model the heat-transfer process in FSP.

References
[1] S. Soleymani, A. Abdollah-Zadeh, S.A. Alidokht // *Materials Physics and Mechanics* **17(1)** (2013) 6.

[2] A. Albakri, S. Aljoaba, M. Khraisheh, *Modelling of Friction Stir Processing with in Process Cooling Using Computational Fluid Dynamics Analysis.* In: Advances in Sustainable Manufacturing, ed. by G. Seliger, M. Khraisheh, I. Jawahir (Springer, Berlin, Heidelberg, 2011) 99. doi:10.1007/978-3-642-20183-7_15.

[3] Y.X. Gan, D. Solomon, M. Reinbolt // *Materials* **3(1)** (2010) 329. doi:10.3390/ma3010329.

[4] M. Folea, A. Roman, C. Langlade, D. Schlegel, E. Gete, D. Chamoret, *Producing Nanograin Surface Layers by Friction Stir Processing.* In: Guide for Nanocoatings Technology (Nova Science Publishers, 2015) 333.

[5] R. Mishra, P.S. De, N. Kumar, *Friction Stir Welding and Processing* (Springer International Publishing, 2014) 13-58.

[6] C. Chen, R. Kovacevic // *International Journal of Machine Tools and Manufacture* **43(13)** (2003) 1319.

[7] M. Chiumenti, M. Cervera, C.A. de Saracibar, N. Dialami // *Computer Methods in Applied Mechanics and Engineering* **254** (2013) 353. doi:10.1016/j.cma.2012.09.013.

[8] K.C. Deshmukh, M.V. Khandait, R. Kumar // *Materials Physics and Mechanics* **22(1)** (2015) 86.

[9] R. Selvamani // *Materials Physics and Mechanics* **21(2)** (2014) 177.

[10] M. Song, R. Kovacevic // *International Journal of Machine Tools and Manufacture* **43(6)** (2003) 605.

[11] C. Langlade, A. Roman, D. Schlegel, E. Gete, M. and Folea // *Materials and Manufacturing Processes* **31(12)** (2016) 1565. doi: 10.1080/10426914.2015.1090584.

[12] M. Gruber, N. Lebaal, S. Roth, N. Harb, P. Sterionow, F. Peyraut // *International Journal of Material Forming* **9(1)** (2016) 21.

[13] N.A. Abrosimov, N.A. Novosel'tseva // *Materials Physics and Mechanics* **23(1)** (2015) 66.

[14] A.O. Vatulyan, S.A. Nesterov // *Materials Physics and Mechanics* **23(1)** (2015) 71.

[15] J. Al-Sumait, A. AL-Othman, J. Sykulski // *International Journal of Electrical Power & Energy Systems* **29(10)** (2007) 720.

[16] G.I. Raab, D.V. Gunderov, L.N. Shafigullin, Yu.M. Podrezov, M.I. Danylenko, N.K. Tsenev, R.N. Bakhtizin, G.N. Aleshin, A.G. Raab // *Materials Physics and Mechanics* **24(3)** (2015) 242.